Geomorphology 184 (2013) 38–50

Contents lists available at SciVerse ScienceDirect

Geomorphology

journal homepage: www.elsevier.com/locate/geomorph

Off-river waterbodies on tidal rivers: Human impact on rates of infilling and the accumulation of pollutants

Jonathan D. Woodruff [a,*], Anna P. Martini [b], Emhmed Z.H. Elzidani [a], Thomas J. Naughton [a], Daniel J. Kekacs [b], Daniel G. MacDonald [c]

[a] Department of Geosciences, Univ. of Massachusetts, Amherst, MA 01003, United States
[b] Department of Geology, Amherst College, Amherst, MA 01002, United States
[c] School of Marine Science and Technology, Univ. of Massachusetts, Dartmouth, MA 02744, United States

ARTICLE INFO

Article history:
Received 7 August 2012
Received in revised form 19 November 2012
Accepted 20 November 2012
Available online 28 November 2012

Keywords:
Floodplain
Meander cut-off
Oxbow lake
Sediment transport
Tidal creek
Tie-channel

ABSTRACT

Cut-off meanders, backwater ponds, and blocked valley coves are all common features along the tidal reaches of lowland rivers. While significant progress has been made to understand sediment dynamics in similar off-river environments above the head of tides, less is known about the processes driving transport and sedimentation within these systems when tidally influenced. To provide insight we combine sedimentological observations with flux analyses for a series of tidal off-river waterbodies along the Lower Connecticut River spanning the river's entire 100 km tidal reach. Sedimentation rates exhibit a clear seaward increase with growing tidal influence, and are an order of magnitude higher than accumulation rates obtained previously from neighboring marsh and subtidal environments. A simplified mass balance can relate time-series measurements of water level and suspended sediment concentration to observed trends in sedimentation, and support flood-dominated asymmetry in tidal sediment flux (i.e. tidal pumping) as the primary mechanism for enhanced trapping. Relatively steady rates of deposition are observed in off-river waterbodies over the last century, with little evidence of deposition dominated by extreme events. Suspended sediment concentrations rise significantly in the main tidal river with increasing river discharge, while tidal range is damped with rising freshwater flow. The net result is an optimal freshwater discharge for maximizing the tidal pumping of sediment from the main river into tidal off-river waterbodies, with more routine discharge events largely responsible for driving long-term trends in deposition. A sudden shift in lithology towards more inorganic, fluvial derived sediment is commonly observed towards the end of the 19th century, along with over an order of magnitude increase in the rate of deposition. The timing of the onset of rapid infilling occurs contemporaneous with the documented creation and/or deepening of tidal tie-channels, followed shortly after by a rapid rise in heavy metal concentrations related to industrial activity along the river. Results point to the creation and routine maintenance of tidal inlets increasing the connectivity of off-river waterbodies to the main tidal river in recent centuries, and enhanced sediment trapping along the floodplain at the most favorable time for capturing legacy contaminants introduced during the industrial era.

1. Introduction

Understanding how sediment is transported, trapped, and remobilized in low-lying rivers and their respective estuaries is of broad geomorphic significance, fundamental to quantifying river inputs to the ocean, constraining internal inventories, and predicting the evolution of low gradient landscapes (e.g. Meade, 1982). A great deal of research describes the transport and trapping of sediment along low-lying rivers at locations above the tidal reach (e.g. Allison et al., 1998; Aalto et al., 2008; Day et al., 2008; Swanson et al., 2008), and further downstream within the brackish waters of an estuary (e.g. Geyer et al., 2001; Woodruff et al., 2001; Klingbeil and Sommerfield, 2005; Galler and Allison, 2008; Ralston and Geyer, 2009). By comparison, less is known about the mechanisms for transport and storage between these two environments within the freshwater tidal river, or the perimarine zone (e.g. Hageman, 1969; Plater and Kirby, 2006). This freshwater tidal reach can constitute a significant portion of a low-gradient river's overall extent, particularly for low-lying rivers along the eastern seaboard of North America, where tides frequently extend upriver from the mouth on the order of 100-to-200 km (Fig. 1).

The predominant location for long-term (decadal-to-centennial), fine-grained storage in a river above the head of tides (tidal limit) is often considered to be the floodplain, (e.g. Trimble, 1983; Allison et al., 1998; Goodbred and Kuehl, 1998; Walling et al., 1998, 1999),

* Corresponding author. Tel.: +1 413 577 3831; fax: +1 413 545 1200.
E-mail address: woodruff@geo.umass.edu (J.D. Woodruff).

0169-555X/$ – see front matter © 2012 Elsevier B.V. All rights reserved.
http://dx.doi.org/10.1016/j.geomorph.2012.11.012

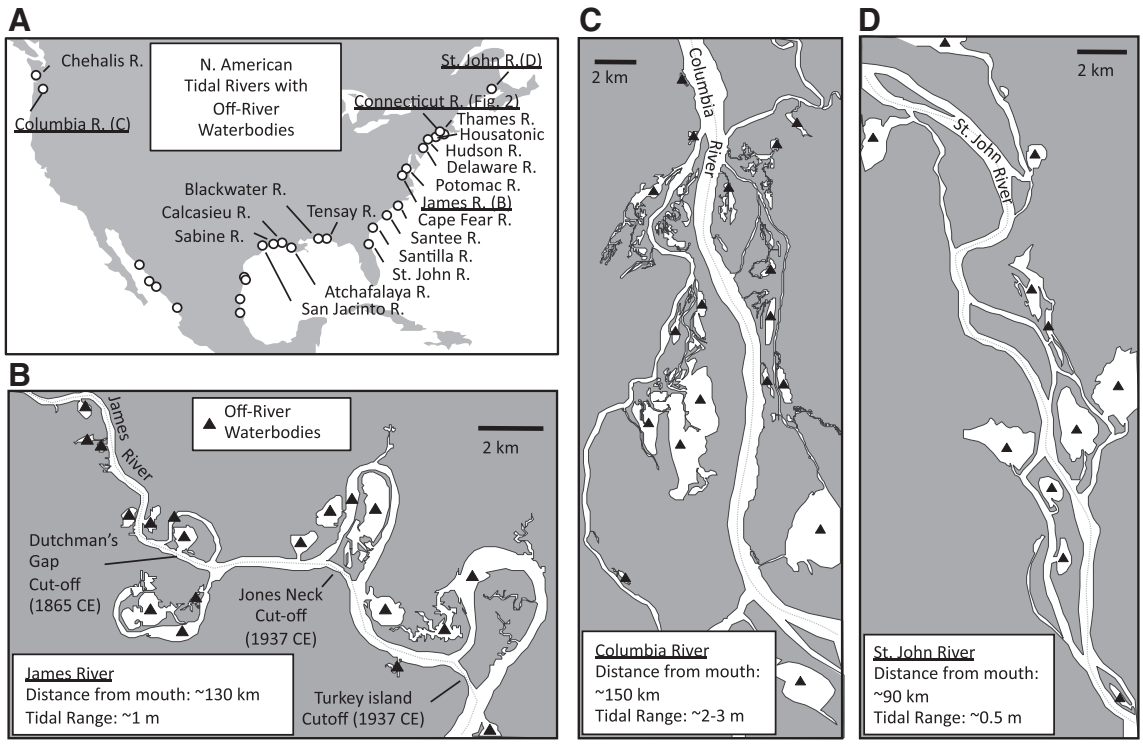

Fig. 1. (A) North American map showing the distribution of tidal rivers with known off-river waterbodies. Portions of rivers underlined in (A) are enlarged in (B), (C), (D), and Fig. 2. Off-river waterbodies in B–D are identified with triangles. A number of the most prominent off-river waterbodies along the James River (shown in B) are man-made, due to navigation cut-offs beginning in the mid-1860s.

where sediment is transported and trapped primarily during seasonal high river discharge events (e.g. Wolman and Miller, 1960; Mertes, 1994; Walling et al., 2003). In contrast, provided that an estuary has sufficient accommodation space, significant amounts of fine-grain sediment can also be trapped and stored within the estuarine channel itself, both seasonally (e.g. Woodruff et al., 2001; Traykovski et al., 2004; Galler and Allison, 2008) and on decadal and centennial time scales (e.g. Klingbeil and Sommerfield, 2005). Similar to locations above the influence of tides, non-ephemeral depocenters of fine-grained sediment within the fresh water tidal reach are generally located along the floodplain rather than the channel itself (e.g. Patton and Horne, 1992; Varekamp et al., 2003), in part because the main channel often lacks the accommodation space required for significant amounts of long-term, fine-grained sediment storage.

Off-river waterbodies, such as cut-off meanders, backwater lakes, and drowned valley coves serve as prominent depocenters for the focused sedimentation of fine-grained sediment along the floodplain, primarily because these systems present significantly more vertical accommodation space than neighboring subaerial wetland environments. These floodplain waterbodies function as unique and essential habitats for flora and fauna (e.g. Simpson et al., 1983), provide sheltered harbors and recreational areas (e.g. Maloney et al., 2001; Jacobs and O'Donnell, 2003), serve as an important sink for nutrients, organic carbon and associated contaminants (e.g. Bubb et al., 1991, 1993; Loomis and Craft, 2010), and are a key ecohydrological component of the perimarine floodplain (e.g. Plater and Kirby, 2006). Critical to managing all of these important functions is an understanding of the mechanisms by which off-river waterbodies infill.

A number of recent papers have provided valuable insight into the processes governing the transport and trapping of material in floodplain waterbodies when located in a strictly fluvial environment (Rowland et al., 2005; Day et al., 2008; Constantine et al., 2010). These works highlight the importance of seasonal discharge events to the infilling of these environments. They also emphasize the significance of tie-channels that connect off-river waterbodies to the main river, and the important role these tie-channels play in diverting sediment loads from the main river to the floodplain.

Off-river waterbodies are also prevalent along the tidal reach of many of low-lying rivers throughout the world, and are particularly prominent along the western Atlantic Slope (e.g. Fig. 1). Here we provide a new empirical data set for understanding how these tidal off-river waterbodies infill. More specifically the study is focused on assessing: i) the relationship between tidal magnitude and rates of infilling, and ii) how human alterations to tidal off-river waterbodies have affected sediment trapping in recent centuries.

2. The Connecticut River

Examples of notable North American rivers that contain prominent tidal off-river waterbodies are presented in Fig. 1 and include (with the length of their approximate tidal reaches in brackets): the Saint John River in New Brunswick, Canada [140 km], the Connecticut River [100 km], the Hudson River [250 km], the Delaware River [200 km], the Potomac River, [164 km], the James River [160 km], the Santee River [60 km], the St. John River in Florida [180 km], the San Jacinto River [260 km], and the Columbia River [220 km]. In particular, the lower reach of the Connecticut River exemplifies a system with prominent tidal off-river waterbodies (Fig. 2). The river has long been recognized for its extended tidal environment, dating back to its early documented history when Native Americans originally referred to the Connecticut as "Quinnetukut," meaning long tidal river (Horne and Patton, 1989). Tides begin at the mouth of the river at Long Island Sound with a semi-diurnal range of 1.1 m, and propagate upstream roughly 100 km to just below Thompsonville, CT (Fig. 2A). A majority of the tidal river is fresh, with the salinity intrusion typically extending up the estuary 5 to 15 km during periods of high and low river discharge, respectively (Garvine, 1975; Howard-Strobel et al., 1996).

Estimates of total fine grain sediment load for the river range from 250,000 tonnes/yr (Milliman and Farnsworth, 2011) to 760,000 tonnes/yr (Patton and Horne, 1992), of which a sizable

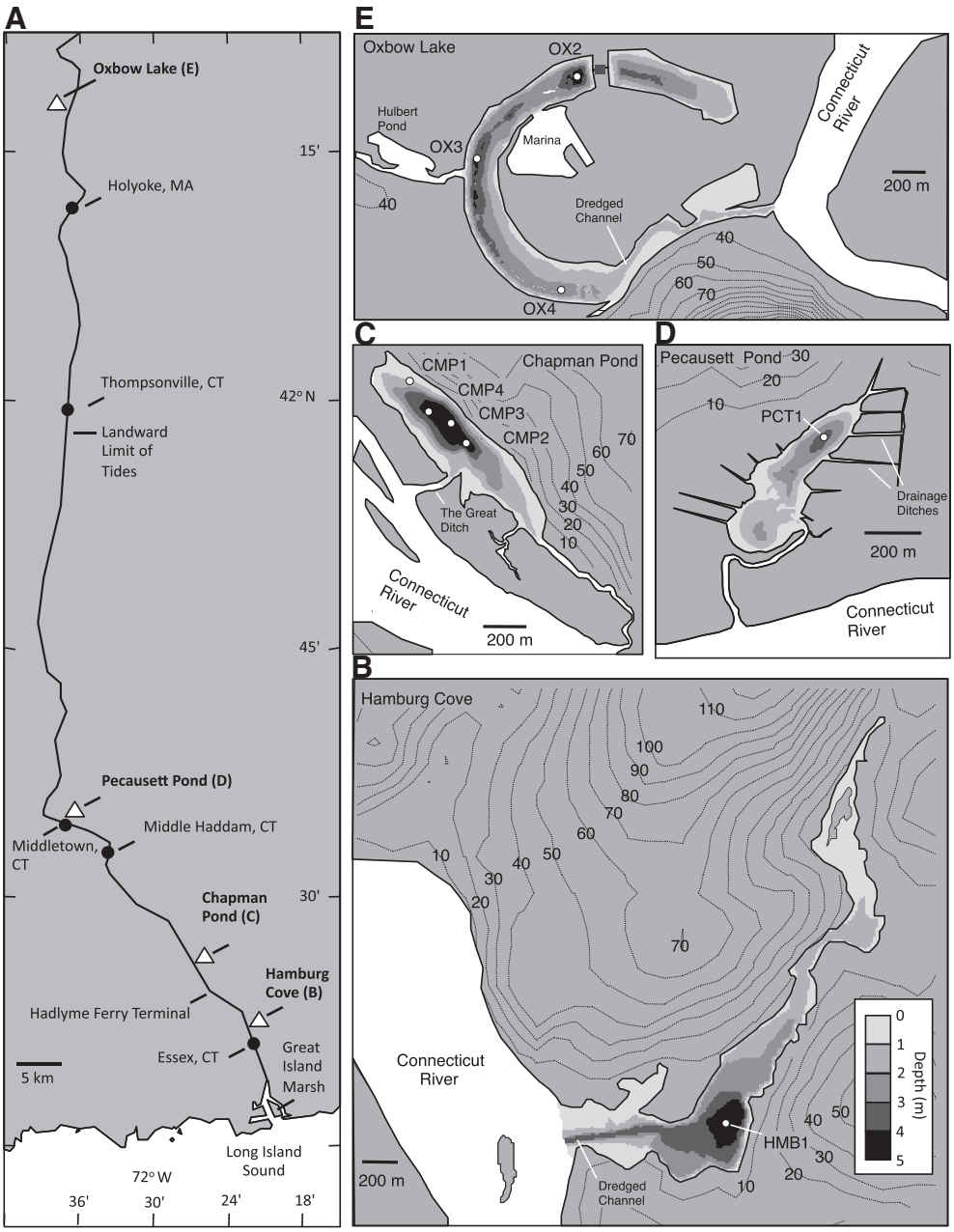

Fig. 2. (A) The Lower Connecticut River and Estuary with location of Hamburg Cove (B), Chapman Pond (C), Pecausett Pond (D) and Oxbow Lake (E). Black circles in A identify United States Geological Survey gauging stations referenced in text. White circle in B–E identify core locations. Contour shading of bathymetry is the same in B through E. The location of the original core collected by Varekamp et al. (2003) is labeled CMP1 in C, with CMP2-4 collected in this study.

fraction (~20%) is trapped and stored within the tidal reach (Patton and Horne, 1992). Relatively minor changes have been observed in the bathymetry of this tidal reach over the last century (Horne and Patton, 1989), indicating that a majority of fines are potentially trapped within adjacent tidal floodplain settings rather than the main channel itself. More recent studies measure roughly 30 cm of deposition since the onset of industrialization within floodplain wetlands on Great Island Marsh (Varekamp et al., 2003, 2005, See Fig. 2 for location), and support the tidal floodplain as a primary location of fine-grained sediment storage.

3. Study sites and history of man-made modifications

The study centers on a 160 km transect composed of four off-river waterbodies along the banks of the Connecticut River, beginning above the tidal reach of the river and continuing down to the mouth of the estuary. Starting near the river mouth where tides are greatest and progressing upriver these sites include Hamburg Cove, Chapman Pond, Pecausett Pond, and Oxbow Lake (Fig. 2).

3.1. Hamburg Cove and channel dredging

Hamburg Cove is situated along the east side of the Connecticut River approximately 13 km from the mouth, and is the most seaward site analyzed in the study (Fig. 2B). The landward limit of salt water is typically located just below the cove, except during periods of low river discharge when the salinity intrusion extends slightly upriver (Horne and Patton, 1989). Tides are the dominant driver of flow in the cove, with mean and spring ranges of approximately 1.1 m and 0.9 m, respectively (NOAA, 2012). A small, dammed tributary (Eightmile River) also feeds into the cove from the east with an average annual discharge of 2.4 m^3/s, and peak annual flows typically

below 60 m^3/s (mean and peak estimates based on combined statistics for north and east branches of the Eight Mile tributary from #01194000 and #01194500 USGS gauging stations).

Hamburg Cove is housed within a narrow, drowned glacial valley with a steep rocky shoreline. The sheltered off-river setting of the cove made it an attractive harbor to early settlers of the region; however, natural sedimentation from the Connecticut River results in a shallow submerged levee at the mouth roughly 0.5 m or less in depth (Fig. 2B). Early records indicate that a navigation channel was either created or deepened in 1909 CE to improve access to the cove (Schuler, 1993). This deeper, 30 m-wide, 3 m-deep tidal channel now cuts through the shallow shoal at the mouth of Hamburg Cove, and currently serves as its primary connection to the Connecticut River. With the exception of this navigation channel, the deeper inner cove appears to have remained relatively untouched prior to sampling, with average depths in the pond's interior ranging from 4 to 5 m.

3.2. Chapman Pond, mercury contamination, and the Great Ditch

Chapman Pond is a 0.24-km^2 freshwater tidal pond located approximately 10 km upstream of Hamburg Cove along the eastern floodplain of the Connecticut River (Fig. 2C). At this location salt is completely absent from the river under all conditions, and the mean and spring tidal range diminish to 0.8 m and 1.0 m, respectively (NOAA, 2012). The elongated pond runs parallel to the river suggesting that it likely occupies a braid cut-off carved previously when the river tracked to the east of its current location. The pond is absent of any major tributaries other than three small streams with a cumulative watershed of less than 2 km^2.

The banks of Chapman Pond are fringed with a vegetated shoal that shallows to a larger tidal freshwater marsh. A network of cores collected previously by Varekamp et al. (2003) for the entire Connecticut River/Long Island Sound region includes a core collected towards the north bank of Chapman Pond along this subtidal shoal (core CMP1, Fig. 2C). Temporal trends in heavy metal deposition in core CMP1 are consistent with trends observed from the larger network of sites obtained by Varekamp et al. (2003). More specifically a rapid rise in mercury (Hg) deposition above background levels dates to sometime at the turn of the 19th century and marks the onset of industrial activity along the river.

Chapman Pond is separated from the Connecticut River by a ~150 m wide, naturally formed channel levee. This forested barrier is intersected by a primary tidal tie-channel feeding into the central west side of the pond, and a longer meandering tidal creek connecting to the pond's southern end (Fig. 2C). The primary, western inlet is a man-made canal called 'The Great Ditch', created and/or deepened by commercial fisherman sometime between the 1850s and 1890s following the blockage of the smaller southern creek by a local land owner to prevent fisherman access to the pond (Maloney et al., 2001). This Great Ditch has been maintained ever since, with the remains of cut tree trunks and limbs along the banks providing evidence for the routine removal of tree jams in order to ensure continued access to the pond.

3.3. Pecausett Pond, drainage ditches and inlet maintenance

Pecausett Pond (also called Wright Pond) is located 43 km from the mouth of the Connecticut River and 20 km upstream from Chapman Pond (Fig. 2D), with mean and spring tidal ranges of 0.7 m and 0.8 m, respectively (NOAA, 2012). The pond is situated along a stretch of the Connecticut River that tracks sharply to the east through the eastern border fault of the Hartford Basin (Horne and Patton, 1989). Bordering Pecausett Pond to the north is a small bedrock valley, potentially carved when the Connecticut River passed to the east of its current path during pre-glacial times (Bissell, 1925). The elongated, 3–4 m deep pond follows this northeast–southwest oriented paleo-river valley, potentially indicating that it is in part a modern expression of this pre-glacial geometry. Alternatively, it is also possible that the pond is a prehistoric cut-off formed when the river meandered into this valley and was pinned against a series of bedrock hills to the north.

Direct freshwater runoff into Pecausett Pond is minimal, with no major streams or tributaries. Similar to Chapman Pond, the deeper interior of Pecausett Pond is bordered by a fringing sub-tidal shoal followed landward by a larger intertidal marsh. An expansive network of drainage ditches have been cut through Pecausett marsh, a common practice for lowering water-tables and draining marsh surfaces for hay farming and later insect control (Bourn and Cottam, 1950; Redfield, 1972; Rozsa, 1995). Historical maps from the region indicate that these ditches were dug sometime between 1859 CE and 1895 CE (Walling, 1859; Duffield, 1895).

A single ~30 m wide, ~1 m deep tidal tie-channel serves as the sole connection between Pecausett Pond and the main Connecticut River (Fig. 2D). This channel has remained roughly in the same location at least as far back as 1859 CE (Walling, 1859), but with older maps insufficient in resolution to assess the prior state of the inlet. Similar to Chapman Pond, evidence of cut limbs and tree stumps along the banks of the inlet to Pecausett Pond at the time of sampling indicate the routine removal of clogging debris for improved access to the pond.

3.4. Oxbow Lake and human modifications

Oxbow Lake is the most upriver site in the study (located approximately 160 km north of the mouth), and the only site that is not influenced by tides (Fig. 2E). The lake was formed in 1840 CE when a wide western meander from the main stem of the river was cut-off during a spring flood (Holland and Burk, 1982). A few years after its creation the northern end of the Oxbow was blocked (Walling, 1856), leaving a 35 m wide channel on the southern end of the lake that remains the sole connection between it and the main river. Manahan River, a small 17.5 km-long tributary, enters Oxbow Lake on the southern end. Since 1940 CE the Mill River, with a mean annual discharge of 2.8 m^3/s and average peak discharges of 71 m^3/s (USGS gauging station #01171500), has also been redirected into the lake, entering along its northwest bank. Since its diversion, Mill River has entered Oxbow Lake by way of Hulbert Pond, an older relic cut-off meander located just to the northeast, with Hulbert Pond continuing to serve as the initial catchment for Mill River sediment prior to entering Oxbow Lake (Holland and Burk, 1982). A marina exists along the north side of Oxbow Lake with the lake's southern outlet maintained in order to ensure navigational access from the lake to the main river (Fig. 2E).

4. Methods

4.1. Field program

Field work for the study consisted of an initial subbottom survey of each of the four off-river waterbodies followed by a coring program guided by these preliminary geophysical profiles. A Mala Ground Penetrating Radar (GPR) operating at 50 to 250 MHz was used to collect bathymetry and preliminary subbottom stratigraphy for Oxbow Lake, Pecausett Pond and Chapman Pond, with seismic surveys for the seasonally brackish Hamburg Cove site obtained using an acoustic profiler operating at 10 KHz.

Once targeted with subbottom surveys and derived bathymetry, sediment cores were collected at the deepest location within each waterbody. In addition to these primary core sites, a transect of additional cores was also obtained from Chapman Pond and Oxbow Lake in order to assess spatial variability in deposition within these individual

waterbodies (Fig. 2B–E). Long cores were obtained using a combination of piston-push coring (e.g. Donnelly and Woodruff, 2007; Woodruff et al., 2008, 2009) and vibra-coring (Boldt et al., 2010) techniques.

4.2. Lab methods

Gravimetric porosity and loss-on-ignition measurements follow methods described by Dean (1974). Sub-sampled sediments were weighed and dried overnight at 105 °C. Dried samples were reweighed and combusted at 550 °C for 2 hrs to determine the organic mass lost. Grain-sizes were measured on surface sediments using a Coulter LS 200 laser particle size analyzer, with organics removed using 6% H_2O_2 at ~60 °C prior to analysis. Statistical data was computed using the Fraunhofer optical model with the median grain size (i.e. D_{50} by volume) provided to characterize surficial sediment size.

Hg measurements were obtained with a Teledyne Leeman Labs Hydra-C mercury analyzer at Amherst College. The Hydra-C is a direct combustion Hg analyzer with cold vapor atomic absorption configuration (CVAAS). Dried and weighed samples were combusted and mercury collected onto a gold amalgamation trap before being released into the CVAAS. National Institute of Standards and Technology (NIST) sediment standard 2702 (inorganics in marine sediment) was used for calibration and to determine precision and accuracy, where precision was within 2% and accuracy was +/−8%.

4.3. Chronostratigraphic techniques

Age models for selected cores were obtained using a combination of dating techniques including gamma spectroscopy, Hg stratigraphy, and radiocarbon dating. For radioisotope analysis powdered sediment were counted on a Canberra GL2020R Low Energy Germanium Detector for 24–48 h. The initial rise and subsequent peak in ^{137}Cs activities are well proven age markers for the 1954 CE onset and 1963 CE peak in atmospheric nuclear testing, respectively (Pennington et al., 1973), with measurements of unsupported ^{210}Pb activities ($t_{1/2}$ = 22.3 yrs) providing further age constraints. Activities for ^{137}Cs and ^{210}Pb were computed spectroscopically from the 661.66 keV and the 46.54 keV photopeaks, respectively.

Excess or unsupported ^{210}Pb activities ($^{210}Pb_{ex}$) were obtained using the difference between total ^{210}Pb activity and the in situ ^{226}Ra supported ^{210}Pb activity as measured by ^{214}Pb (e.g. Chen et al., 2004). Average rates of sedimentation based on $^{210}Pb_{ex}$ were estimated using the best-fit linear regression for the logarithm of $^{210}Pb_{ex}$ versus depth (Koide et al., 1973; Robbins and Edgington, 1975; Faure, 1986), with the slope of this best-fit line equivalent to $-\lambda/r$, where r is the sedimentation rate and λ is the radioactive decay constant of ^{210}Pb (0.03114 yr^{-1}). Discrete ages for individual $^{210}Pb_{ex}$ measurements were obtained with the age-to-activity relationship described by Appleby and Oldfield (1978) when assuming a constant initial concentration (CIC) of $^{210}Pb_{ex}$:

$$t = \frac{1}{\lambda} \ln \frac{C_o}{C_x}. \quad (1)$$

Here C_o is the activity of $^{210}Pb_{ex}$ at time t_o, and t is the age relative to t_o for sediment that has decayed to an activity of C_x.

To extend dating beyond ^{137}Cs and $^{210}Pb_{ex}$ chronologies, accelerated mass spectrometry ^{14}C analyses were also conducted on organic samples at the National Ocean Science Accelerator Mass Spectrometry Facility at Woods Hole Oceanographic Institution. Resulting radiocarbon ages were calibrated to calendar years with associated analytical error using the IntCal09 (Reimer et al., 2009) calibration data set.

In addition to the deeper cores obtained to derive longer-term deposition rates, a series of short gravity cores were also collected in the late-spring of 2011 to assess rates of deposition during a series of fairly routine high-river discharge events associated with the year's seasonal spring meltwater event (i.e. spring freshet). All sediments obtained via gravity core were sub-sampled in the field at 0.5–1.0 cm depth intervals to avoid disruption. The depth of detectable ^{7}Be activity in these sediments was then employed as a marker of seasonal deposition, with ^{7}Be activities determined by gamma spectroscopy of the 477.6 keV photopeak following previously reported methods (Larsen and Cutshall, 1981).

^{7}Be is a short-lived cosmogenically derived radio-isotope ($t_{1/2}$ = 53 days) that is delivered to the surface of the Earth primarily by precipitation (Feng et al., 1999; Olsen et al., 1986). Suspended fine-grained sediments readily scavenge ^{7}Be from the water column of rivers that contains fresh rainwater (e.g. Olsen et al., 1986). Following deposition ^{7}Be activities within these previously suspended sediments rapidly decay below the limits of detection, with the depth of measurable ^{7}Be activity often used as an effective marker for sediments deposited within roughly three half-lives or approximately the last 6 months (Walling, 2003). To assess overall infilling rates of waterbodies results are presented as the thickness of detectible Be^7 (i.e. cm or cm^3/cm^2) rather than the mass accumulation rate (i.e. $g/cm^2/yr$).

5. Results

5.1. Deposition rates over the last century

Sedimentological results from Hamburg Cove are based on HMB1, a 550 cm core collected from the deepest region of the cove's central interior (water depths of roughly 4 to 5 m), and at a horizontal distance of roughly 360 m to the east of the navigation channel that connects the cove to the main river (Fig. 2B). The 1954 CE ^{137}Cs onset is observed between a sediment depth of 200 and 240 cm in the HMB1 core followed by a clear 1963 CE peak in ^{137}Cs activity at 181 cm (Fig. 3A). An average sedimentation rate of between 3.6 and 4.3 cm/yr is obtained for HMB1 based on the depth of these two separate chronological controls. Independent age constraints derived from $^{210}Pb_{ex}$ activities are consistent with this ^{137}Cs chronology, with the best-fit $^{210}Pb_{ex}$ decay curve indicating a relatively steady deposition rate of 4.2 cm/yr since the late 1930s (Fig. 3E, I).

Similar to HMB1, CMP2 was obtained from the deepest section of Chapman Pond in water depths of 4 to 5 m, but at a somewhat closer distance of ~160 m from the pond's main inlet. The 1954 CE onset for ^{137}Cs activity in CMP2 occurs between 166 cm and 180 cm, with a 1963 CE ^{137}Cs peak at 151 cm (Fig. 3B). A sedimentation rate of roughly 3.0–3.2 cm/yr is obtained with these ^{137}Cs ages, and similar to the rate of 3.1 cm/yr obtained using the best-fit decay curve for $^{210}Pb_{ex}$ activities (Fig. 3F, J).

Sediment analyses from the most landward tidal pond in the study (Pecausett Pond) are focused on PCT1, a core collected from the pond's deepest point in 3 to 4 m of water and approximately 350 m away from the tidal inlet (Fig. 2D). A well-defined 1963 CE peak in ^{137}Cs activity is presented in PCT1 at a sediment depth of between 80 and 82 cm, followed below by the 1954 CE onset of ^{137}Cs activity between 108 and 115 cm (Fig. 3C). Sedimentation rates based on this ^{137}Cs chronology are between 1.7 and 2.1 cm/yr, with the best-fit decay curve for $^{210}Pb_{ex}$ also reveals a similar rate of 2.1 cm/yr over the last half century (Fig. 3G, K).

Above the head of tides at Oxbow Lake, short-lived radioisotopic activities were measured in core OX2, located approximately 2000 m from the main inlet and in a water depth of approximately 4 to 5 m (Fig. 2E). ^{137}Cs age constraints are at the shallowest sediment depths of all the four core sites, with the 1963 CE peak at 55 cm and the 1954 CE onset of ^{137}Cs activity at a depth of ~84 cm (Fig. 3D). Sedimentation rates at OX2 based on these age constraints are between 1.2 and 1.5 cm/yr, with the best-fit $^{210}Pb_{ex}$ curve also supporting a similar sedimentation rate of 1.5 cm/yr over the last century (Fig. 3H, L).

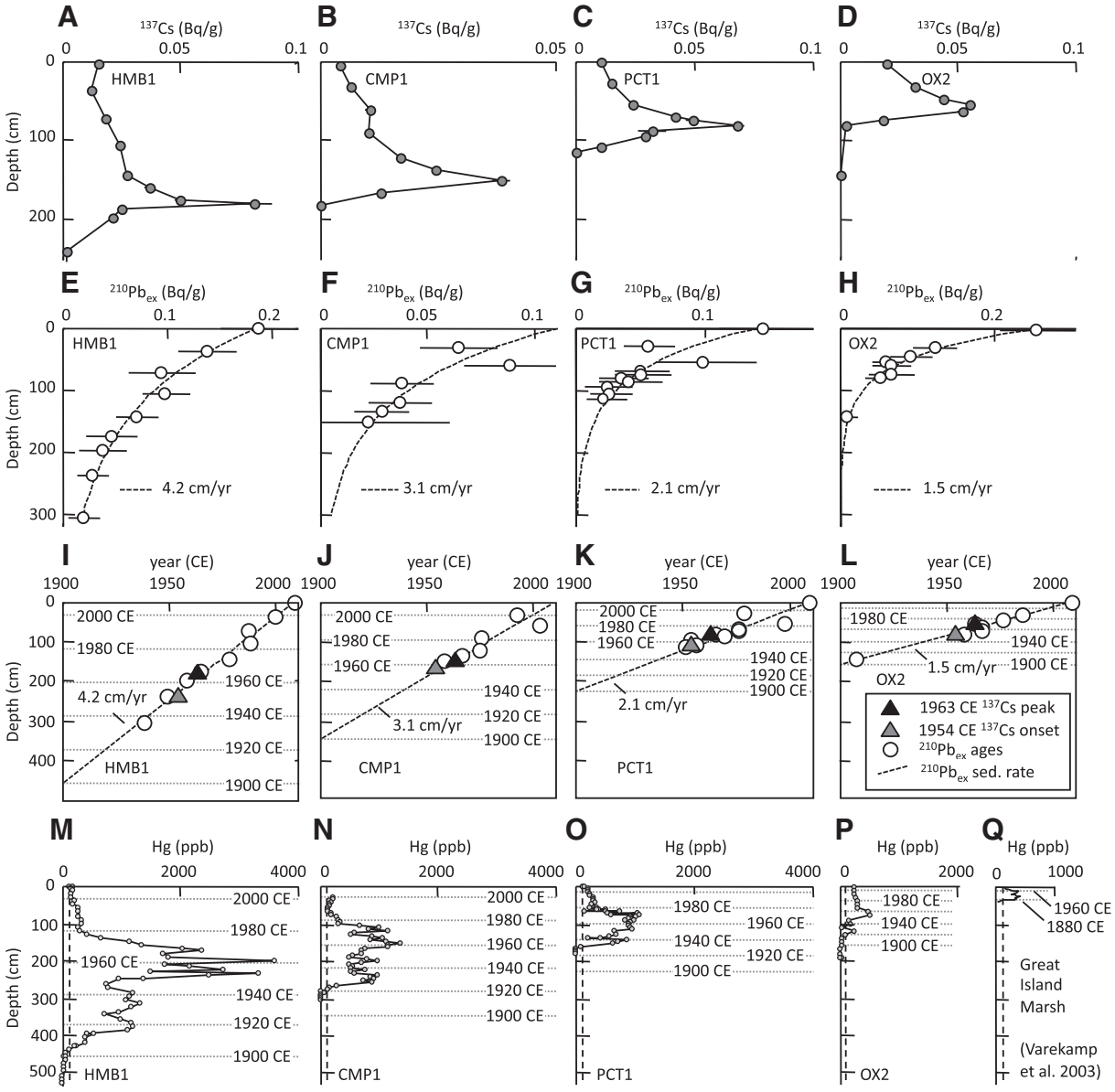

Fig. 3. Sediment depth profiles of ^{137}Cs activity (A–D) and ^{210}Pb$_{ex}$ activity (E–H) along with derived depth-to-age models (I–L). Columns from left to right are for cores HMB1, CMP2, PCT1 and OX2, respectively. Hg concentration for cores are shown in bottom panels (M–Q), with previous data from Great Island Marsh at lower right (from Varekamp et al., 2003). Vertical black dashed lines in Hg profiles identifies upper bound for Hg concentrations that occur naturally in regional sediments (Varekamp et al., 2003). Years presented in M–P are based on the depth-to-age models derived in I–L, with ages in Q from age model by Varekamp et al. (2003).

5.2. Hg chronologies

Industrial waste is an unwanted legacy of centuries of development along the banks of urbanized river systems. Among the most toxic of these contaminants is mercury (a known neurotoxin to humans and wildlife) whose concentrations readily mark industrialization of the Connecticut River watershed (e.g. Varekamp et al., 2003). Regional surveys of floodplain wetlands show natural levels of Hg ranging between 23 and 103 ppb for sediments deposited prior to industrialization (Varekamp et al., 2003), a finding consistent with previous baseline concentrations in sediments (Reimers and Krenkel, 1974). A rapid rise in Hg is observed at all four core sites above these background levels (Fig. 3M–P). This initial rise in Hg consistently dates to sometime between 1900 CE and 1930 CE when more recent ^{137}Cs- and ^{210}Pb$_{ex}$-derived rates of deposition are assumed constant down to this heavy metal horizon. Chronologies developed previously by Varekamp et al. (2003) from a marsh nearby to Hamburg Cove (i.e. Great Island Marsh, see Fig. 2A for location), date this onset of industrial-related Hg to a slightly older age of 1880 CE (Fig. 3Q). An age of between 1900 CE and 1930 CE is still generally consistent with these previous results given dating uncertainties (e.g. ^{210}Pb$_{ex}$ levels primarily used for dating this Hg horizon begin to approach the detection limit in material deposited towards the turn of the 19th century). Later, and better temporally constrained patterns in Hg deposition are more consistent between floodplain waterbodies and past marsh reconstructions. For example, HMB1, CMP2, PCT1 and OX2 all contain a prominent peak in Hg concentration that dates to between 1950 CE and 1970 CE (Fig. 3M–P), which is temporally consistent with the timing of a similar Hg peak observed previously at Great Island Marsh (Fig. 3Q).

Although the timing is similar, the magnitude of the more recent 1950–1970 CE Hg peak is significantly greater in the floodplain waterbodies than in nearby marsh environments. For example, Hg concentrations exceed 3600 ppb at Hamburg Cove, compared to a

maximum Hg concentration of just 409 ppb at Great Island Marsh (Fig. 3M, Q). The onset of industrial-related Hg contamination also extends down to significantly greater depth within floodplain waterbodies when compared to neighboring marshes, with the Hg pollution marker found at a depth of 443 cm at Hamburg Cove, compared to a depth of just 30 cm at Great Island Marsh.

5.3. Spatial trends in Hg deposition at Chapman Pond

Beginning at the core site closest to the main tidal inlet and progressing north, the along-axis transect of cores collected from the deepest section of Chapman Pond include CMP2, CMP3, and CMP4, with respective distances of 160 m, 280 m and 400 m away from the main tidal inlet. The onset of industrial-related Hg contamination in Chapman Pond extends down to similar depths of 276 cm at CMP2 (Fig. 4D) and 294 cm at CMP3 (Fig. 4C), followed by a slight shallowing of this heavy metal horizon to a sediment depth of 247 cm at CMP4 (Fig. 4B). The depth of this heavy metal horizon then decreases significantly when progressing onto the shallower, vegetated shoal to just 43 cm at core CMP1 (Fig. 4A). Hg results from Chapman Pond therefore support roughly the same rates of deposition for the deeper central region of the pond over the last century at CMP2 and CMP3, with a slight decline in sedimentation at the more distal CMP4 core site, followed by a much more rapid decrease in sedimentation over the shallower subtidal banks of the pond.

5.4. Spatial trends in Hg deposition at Oxbow Lake

Above the head of tides at Oxbow Lake, age constraints from core OX2 are at the shallowest sediment depths of all the four study sites (Fig. 3). However, OX2 is located roughly 2000 m away from where the Connecticut River inlet enters Oxbow Lake, and at a significantly greater distance to the main river when compared to core sites from Pecausett Pond, Chapman Pond and Hamburg Cove (e.g. Fig. 2B–E). Core OX4 is located roughly 330 m from where the lake's maintained tie-channel enters into its deeper interior. HMB1 and PCT1 are located at a similar distance from their respective inlets. A spacing of 330 m also reflects a distance that is roughly in between cores CMP3 and CMP4 at Chapman Pond, with Hg profiles from CMP3 and CMP4 indicating similar rates of deposition (Fig. 4C, D).

The industrial Hg horizon is observed to deepen somewhat to a sediment depth of 163 cm at OX4 and 180 cm at OX3, compared to 130 cm at OX2 (Fig. 4E–G). Rates of sedimentation are therefore observed to increase towards the Oxbow Lake inlet. However, this increase is rather gradual and indicates sedimentation rates of between 1.2 cm/yr and 2.0 cm/yr within the lake's deeper interior (assuming the onset of Hg contamination occurred sometime in the early 1900s).

5.5. Seasonal rates of deposition

Detectible ^{7}Be activities increased at HMB1 from a depth of between 0.5 cm and 1.0 cm at the beginning of the 2011 freshet to a depth of between 3.0 cm and 3.5 cm following the freshet (Fig. 5A). This observed increase in depth of measurable ^{7}Be activity at HMB1 when progressing through the spring freshet indicates net accumulation during the event, and supports the use of ^{7}Be in constraining seasonal deposition at the three additional sites. Continuing upriver, ^{7}Be activities extend down to a depth of between 2.5 and 3.0 cm in sediments collected from Chapman Pond at the end of the 2011 spring freshet (Fig. 5B). The depth of detectible ^{7}Be then decreases to depths of between 1.0 and 1.5 cm in freshet sediments collected both from Pecausett Pond (Fig. 5C) and Oxbow Lake (Fig. 5D).

The magnitude of recent deposition during the 2011 spring freshet based on ^{7}Be activities (on the order of a few cm) is roughly consistent with annual rates of deposition obtained with ^{137}Cs and ^{210}Pb$_{ex}$ chronologies (e.g. Fig. 3I–L). Results therefore support seasonal processes driving longer-term rates of sedimentation. Further, ^{7}Be profiles exhibit similar spatial trends, with an increase in rates of deposition towards the mouth of the river.

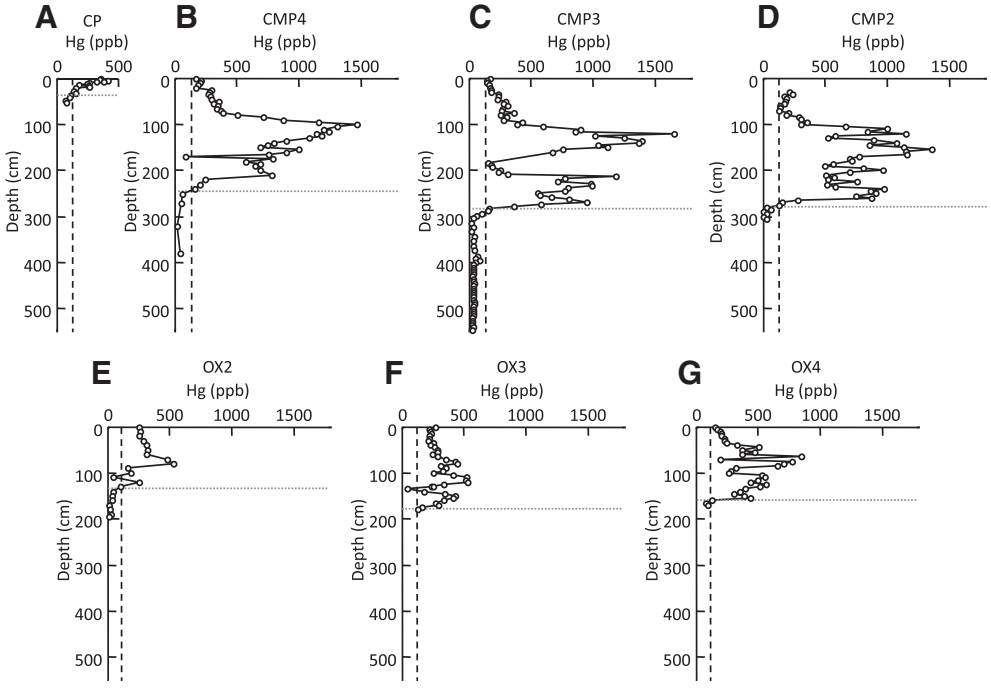

Fig. 4. Hg depth profiles for the transect of cores from Chapman Pond (A–D) and Oxbow Lake (E–G). See Fig. 2C and E for core locations. Gray horizontal line notes the depth when Hg rises above natural levels (black vertical line) as defined by Varekamp et al. (2003).

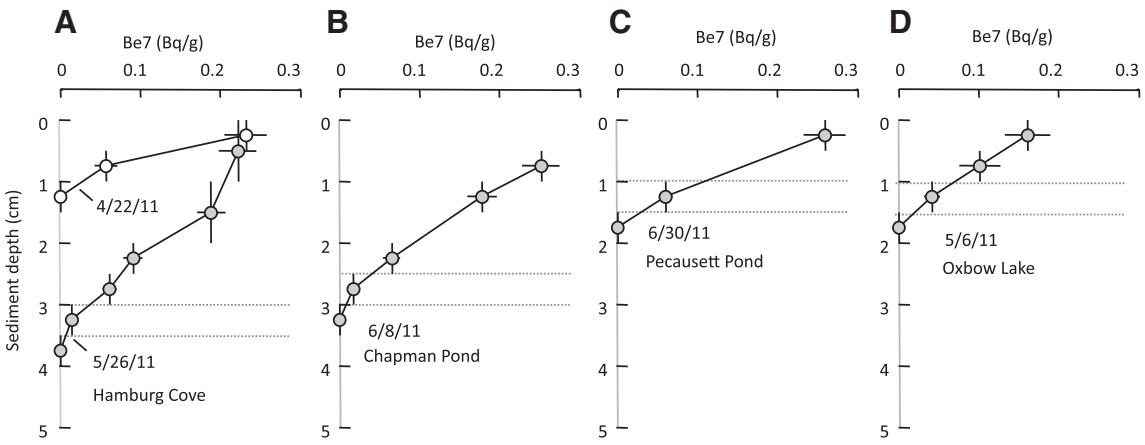

Fig. 5. Depth profiles of ^{7}Be activity. Columns from left to right are from core sites HMB1, CMP2, PCT1 and OX2, with the date of sediment collection noted directly below each profile. Dotted horizontal lines indicate depth-range of detectible ^{7}Be following the 2011 spring freshet.

5.6. Changes in lithology

Loss on ignition (LOI) profiles of organic content from the deepest sediments collected from Chapman Pond at CMP3 reveals relatively high organic content ranging between 20 and 40% (Fig. 6A). Organic content then drops rapidly above a sediment depth of roughly 350 cm (6 ± 1% LOI [1σ]). A comparison of Hg profiles from CMP2 (where ^{137}Cs and ^{210}Pb$_{ex}$ were obtained) and the deeper CMP3 core indicate similar sedimentation rates of 3.0–3.2 cm/yr (Fig. 4C, D). Extrapolating this sedimentation rate back places the sharp 350 cm transition in organic content in CMP3 to sometime in the late 1800s, a date roughly concurrent to the initial opening of 'the Great Ditch' (Maloney et al., 2001).

Trends similar to those in Chapman Pond are also present upstream within a down-core profile of organics from PCT1 at Pecausett Pond (Fig. 6B). A rapid decrease in percent organics is observed above a depth of ~230 cm in PCT1, follow just above by the industrial-rise in Hg at 163 cm (Fig. 6B). A radiocarbon sample obtained below the organic transition in PCT1 at a depth of 240 cm dates to between 1216 CE and 1280 CE (Fig. 6B), and may indicate deposition rates as low as 1 mm/yr for organic sediments deposited prior to the industrial era. It should be noted, however, that radiocarbon ages obtained on organics from the river have the potential to be anomalously old (e.g. Groner et al., 2004), since plant debris can often contain recycled organics that when dated present an older age than the actual time of deposition (the same is potentially true for ^{210}Pb; however, the relative comparison to surficial ^{210}Pb activities in Eq. (1) serves to partly factor out these biases for the shorter-lived radioisotope). The organic matter dated at PCT1 would have to be anomalously old by ~600 yrs to account for discrepancies in rates of deposition above and below the organic transition, which seems unlikely for the fragile leaf matter used for dating. Even when potential ^{14}C reservoir effects are accounted for (e.g. Buck and Millard, 2004), results therefore still point to a dramatic increase in rates of deposition within the last ~100 years at PCT1.

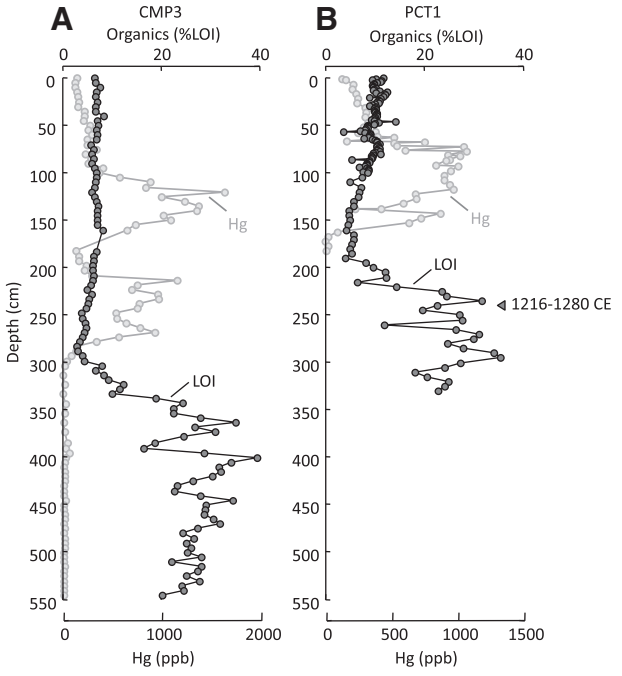

Fig. 6. Depth profiles of organic content (black) based on percent loss on ignition (LOI), and Hg (light gray), for core CMP3 (A) and PCT1 (B). Triangle in B identifies radiocarbon age obtained from PCT1.

6. Discussion

6.1. Tidal pumping

Similarities between the amount of deposition during the 2011 spring freshet obtained using short-lived ^{7}Be, and the magnitude of average annual sedimentation based on longer-lived ^{137}Cs and ^{210}Pb$_{ex}$ activities (both on the order of a few cm/yr), indicate that processes governing the deposition of sediment during the spring freshet of 2011 probably also drive annual-to-decadal deposition rates. An assessment of trapping mechanisms occurring during the 2011 spring freshet therefore provides insight into longer-term trends in accumulation. The depth of detectable ^{7}Be activity is often used as a marker for sediments deposited within roughly three half-lives or approximately the last 6 months (Walling, 2003). Based on this assumption we present cumulative mass flux calculations for the predicted magnitude of deposition at our four study sites between January and July of 2011, using observations of water elevation and suspended sediment concentration obtained along the Connecticut River during this period.

Porosity and grain size characteristics for surficial sediments collected following the 2011 spring freshet are presented in Table 1. Median surficial grain sizes range between 14 and 15 μm, corresponding to a settling velocity of ~0.2 mm/s (Ferguson and Church, 2004). Based on this settling rate, the time scale for settling within a 3–4 m deep pond is ~4–6 h. Grain size analyses therefore suggest that the sediments accumulating within the study's tidal off-river waterbodies are capable of being trapped on the tidal time scale.

Table 1
Sedimentary characteristics for surface sediments collected following the 2011 spring freshet.

Core Site	Porosity	Median grain size (μm)	Organic fraction (%LOI)
OX2	95%	14	15
PCT1	91%	15	12
CMP2	94%	15	9
HMB1	93%	14	15

A rough approximation for the total change in bed elevation during a flooding event (either during a flooding tide or a high river discharge event), can be estimated with the following mass balance:

$$\Delta\eta_{flood} = \frac{\Delta h_{flood} C_{ssc}}{\rho_{sed}(1-n)}. \quad (2)$$

The above is a modification of the Exner equation of sediment continuity (Paola, 2005), where $\Delta\eta_{flood}$ is the change in bed elevation in response to a rise in water level of Δh_{flood}, and C_{ssc} is the suspended sediment concentration observed in the main river, with ρ_{sed} representing sediment density and n the porosity at the bed. The equation assumes that all suspended sediments transported from the river to an off-river waterbody via tie-channels are trapped and evenly distributed along the bed and that sediment concentrations do not vary over the interval of Δh_{flood}. This is probably an oversimplification of bed accumulation in many cases given observed heterogeneities in trapping related to both water depth, tie-channel geometry, proximity to the main inlet, and time-varying changes in C_{ssc} (e.g. Citterio and Piègay, 2009). However, core sites where rates of deposition are assessed are either at roughly the equivalent distances to the site's respective main inlet (i.e. HMB1 and PCT1), or at a location where core transects indicate similar rates of deposition to sites where derived age chronologies are obtained (i.e. CMP2 and OX2, Fig. 4). Thus Eq. (2) seems reasonable in providing a general prediction for relative patterns in deposition between off-river waterbodies based on standard time-series measurements of water level and suspended sediment concentrations collected from the main river.

Water level observations of Δh_{flood} on an interval of every 5–15 min are available from a series of United States Geological Survey (USGS) gauging stations along the lower Connecticut River during the 2011 spring freshet (see Fig. 2A for locations). Above the head of tides at Oxbow Lake Δh_{flood} is approximated using measurements from a gauge nearby at Holyoke, MA. For Pecausett Pond we use staging date collected at a USGS gauging station located directly across the river at Middletown, CT. An additional gaging station located 2 km downstream of Hamburg Cove at Essex, CT provides measurements of Δh_{flood} at this most seaward site. Chapman Pond is situated roughly half way between gauging stations at Middle Haddam, MA and Essex, CT (Fig. 2A), with estimates for Δh_{flood} at this location based on the average water elevation from the two time-series following the application of a 1.9 hour offset that accounts for the average signal lag between the two stations (NOAA, 2012).

Previous water column measurements collected along the Connecticut River just above the head of tides at Thompsonville, CT yield a reasonable power-law relationship between freshwater discharge and C_{ssc} (Fig. 7). Inconsistencies may exist for this types of rating curves (e.g. Nash, 1994; Milliman and Farnsworth, 2011), particularly for extreme precipitation in the uplands of the Connecticut River watershed (Kratz et al., 2012). However, the standard power-law fit between freshwater discharge and suspended sediment concentration has been found effective for discharge events spanning typical seasonal variability, and in predicting spring freshet sediment loads for the neighboring Hudson River (e.g. Woodruff, 1999; Woodruff et al., 2001). Previous suspended sediment concentrations measured towards the mouth of the river near Hamburg Cove are also similar to those predicted above

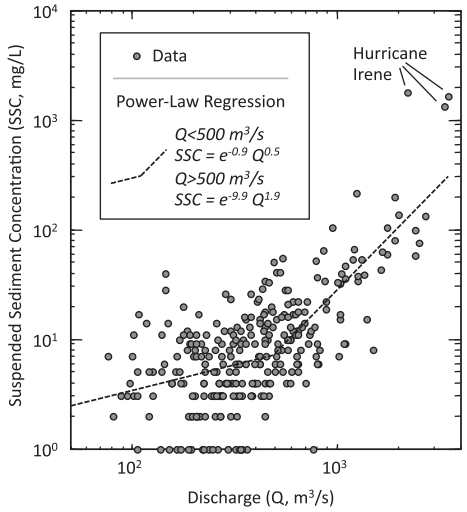

Fig. 7. Log-log plot of USGS mean daily river discharge and sediment load data collected at Thompsonville, CT (See Fig. 1A for location). Dashed line represents the best-fit power-law regressions for low and high discharges following methods described in Woodruff (1999). The increase in slope for the power-law regression at 500 m^3/s is common for rivers in the Eastern United States, and is potentially due to the exposure of more easily erodible material by the removal of bed armoring and the destruction of bank stabilizing vegetation during high flows (Nash, 1994). Suspended sediment concentrations during the three days of peak flow during flooding by Hurricane Irene in 2011 are notes.

the head of tides at Thompsonville (e.g. Fig. 8), suggesting that the non-tidal rating curve presented in Fig. 7 provides a broad approximation for daily average suspended sediment concentrations (i.e. C_{ssc}) throughout the tidal river. Finally, a siliciclastic sediment density of 2650 kg/m^3 is assumed in Eq. (2) given the relatively low fraction of organics observed in freshet sediments (≤15%, Table 1), as well as a representative porosity of 93% (Table 1).

Fig. 9 provides the predicted cumulative time-series of total bed aggradation between January and July of 2011 at each of the four study sites based on the methods described above. The analysis predicts slightly greater than 1 cm of total sedimentation at Oxbow Lake and Pecausett Pond, followed by roughly 2.5 cm in Chapman Pond, and just below 4 cm in Hamburg Cove. These predicted rates of accumulation at each of the four off-river waterbodies are notably similar to measured accumulation during the 2011 spring freshet base on ^{7}Be activities (Fig. 9B), both pointing to a general increase

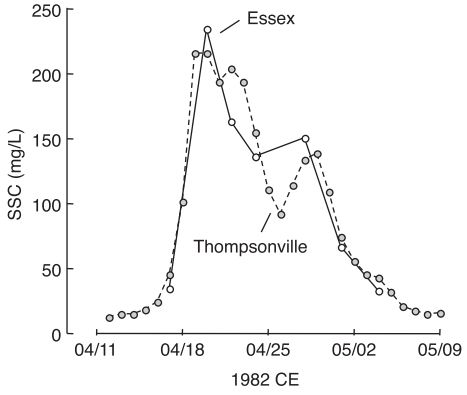

Fig. 8. Time-series of daily averaged suspended sediment concentrations collected near the mouth of the Connecticut River near Essex, CT (solid line) compared to concentrations predicted above the head of tides at Thompsonville, CT (dashed line). Essex data collected by Lemieux (1983). Thompsonville results derived from USGS discharge data in combination with the rating curve shown in Fig. 7.

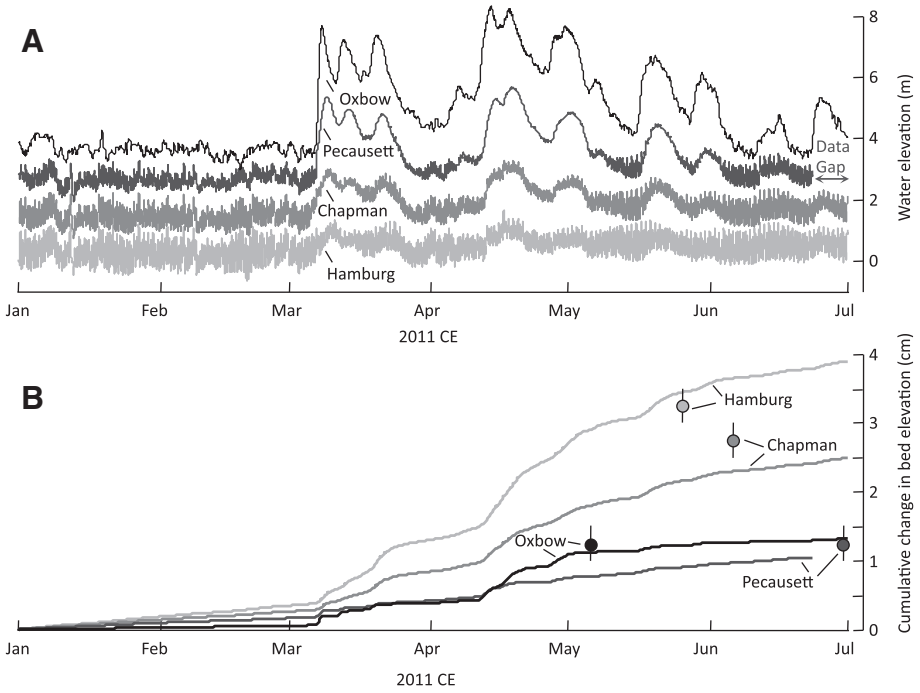

Fig. 9. (A) Water elevations estimated for off-river waterbodies through the 2011 spring freshet. For clarity the mean water level of each time-series has been offset by a constant value. (B) Calculated time-series of bed elevation for respective off-river waterbodies (see text for methods in obtaining results in A and B). Circles identify the timing and depth of detectably ^{7}Be in surface samples collected towards the end of the spring freshet (Fig. 5).

in the trapping of sediment in off-river waterbodies with growing tidal influence (e.g. Figs. 3, 5, and 9B).

The relative importance of tidal processes in introducing fine-grained suspended material into backwater environments from tie-channels can be appreciated when comparing diurnal oscillations in water level within the tidal reach of the Connecticut River to the elevated water levels observed during high river discharge events in upstream segments of the river above the influence of tides (e.g. Fig. 9A). During the 2011 spring freshet the highest relative rise in water level recorded on the Connecticut River above the tidal reach near Oxbow Lake at Holyoke, MA was a little over 4 m. This rise in water is only 4 times the tidal range typically experienced diurnally at the mouth of the estuary at Essex, CT near Hamburg Cove. Periods of elevated discharge extend for a number of days during the 2011 spring freshet. During this flood period the influx of suspended sediment to non-tidal ponds occurs only once during the brief rising stage of the river, with an increase in elevation of just a few meters. In comparison, tidal ponds and coves toward the mouth of the river during the same flood experience oscillations in water height on the order of a meter twice daily, allowing these tidal systems to continually pump suspended sediments from the main river into off-channel waterbodies during each flood tide throughout the entire freshwater discharge event. A similar process of tidal pumping (i.e. the asymmetry in tidal sediment flux) has been recognized as an important driver of transport within the main channel of estuarine systems (e.g. Geyer et al., 2001). The results presented here also highlight tidal pumping as an important driver of transport and trapping to off-channel waterbodies in freshwater tidal rivers.

6.2. Optimal conditions for trapping

The importance of tidal pumping within the Connecticut River indicates that periods of extreme discharge may not provide the ideal conditions for trapping within off-river waterbodies. This interpretation is supported by rates of deposition at study sites remaining relatively steady over the last century (Fig. 3), with little evidence for thick sedimentary units of similar age that would point to sedimentation driven episodically by extreme events. Eq. (2) demonstrates that the product of suspended sediment concentration and tidal range should serve as a proxy for tidal sediment influx to a floodplain waterbody. The product of the lower Connecticut River's suspended sediment rating curve and the best-fit curve relating freshwater discharge to tidal range at the Middletown, CT gauge (nearest to Pecausett Pond) therefore provides an estimate of trapping conditions at Pecausett Pond with respect to freshwater discharge (Fig. 10).

As freshwater flow increases in the river, the tidal reach shortens and is pushed closer to the mouth. Therefore, unlike the positive relationship between suspended sediment concentration and river discharge (e.g. Fig. 10A), the tidal range in the lower river is damped significantly with increased freshwater flow (Fig. 10B). During peak freshwater discharge, although suspended sediment concentrations in the main river are high, tides are small, limiting the magnitude of the term on the right hand side of (2), and indicating a reduced flux of sediment to off-river waterbodies via tidal pumping. This tidal damping effect is particularly prominent at points towards the head of tides (e.g. Pecausett Pond). For example, optimal tidal trapping conditions at Pecausett Pond occur at a discharge of roughly 1000 m^3/s (Fig. 10), well below the average annual peak discharge for the river (2900 m^3/s).

Tides closer to the mouth of the river at Chapman Pond and Hamburg Cove remained relatively unaffected during the 2011 spring freshet (Fig. 9A), indicating that trapping due to tidal pumping continued at these more seaward sites throughout the moderate spring discharge event. However, during periods of extreme discharge tidal effects also diminish significantly at points closer to the mouth, damping sedimentation at these further seaward sites. Instrumental measurements of river stage in the lower tidal river during periods of extreme discharge are limited; however, first-hand accounts provide support for significant tidal damping during periods of abnormally high freshwater flow. For instance, extreme flooding associated with the passage of Hurricanes Connie and Diane in 1955 CE left a watermark approximately 4 m above sea-level 8 km upstream from

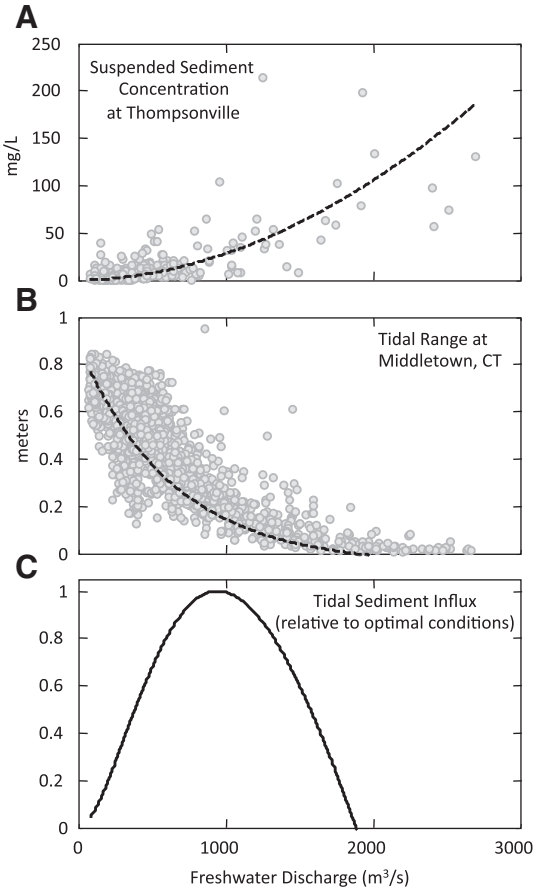

Fig. 10. (A) Suspended sediment rating curve at Thompsonville, CT (same as in Fig. 7 but now plotted linearly). (B) Tidal range at Middletown, CT as a function of freshwater discharge at Thompsonville. (C) Calculated tidal sediment influx into a tidal floodplain water body adjacent to the Middletown gauge (i.e. Pecausett Pond, Fig. 1D) based on the product of the two fitted curves shown in A and B, and normalized to maximum tidal influx.

Hamburg Cove at the Hadlyme Ferry terminal (see Fig. 2A for location). This rise in water would probably have resulted in significant dampening of tides at Hamburg Cove during the event. Similar rates in deposition based on both the 1954 CE onset and the subsequent 1963 CE peak in ^{137}Cs activities at Hamburg Cove support this interpretation of diminished trapping efficiency during the 1955 CE flood, with little evidence for a substantially thicker deposit associated with the 1955 CE flood when compared to resultant deposition from more moderate floods like the 2011 spring freshet (e.g. Figs. 3 and 5).

It is worth noting that although the magnitude of deposition in off-river waterbodies during extreme flooding is likely no greater than more routine seasonal discharge events, the characteristics of this sedimentation by high-magnitude events can be compositionally distinct. For instance, record-breaking discharges in upland tributaries to the Connecticut River during Hurricane Irene in 2011 were sufficient to exceed the threshold for mobilizing fine-grained sediments within glaciolacustrine and lower till deposits, greatly enhancing the supply of glacial fines from these upland landscapes to the main river. When compared to sedimentation from the preceding 2011 spring freshet, resultant deposition from Hurricane Irene was not significantly greater in magnitude, yet found to be anomalously low in organics, finer grained, and exhibiting higher K/Zr ratios, with this unique sedimentary imprint consistent with the enhanced fluvial supply of glacial fines from upland tributaries during extreme precipitation by the Irene event (Kratz et al., 2012).

6.3. Human-induced infilling

Typical depths within tidal off-river waterbodies in this study range from 3 to 5 m. The observed rates of deposition of 2–4 cm/yr therefore cannot be sustained very long without infilling of the entire waterbody. Many of the off-river waterbodies in tidal rivers are formed through the cut-off of old river meanders (i.e., oxbow systems) providing a mechanism for the cyclic creation of these off-river environments. Tie-channels may also open and close due to natural processes even before an individual pond might become maximally infilled. It seems fortuitous, however, that all of the active tidal backwater environments considered in this study should exist at roughly the same stage of infilling.

The observed shift to more clastic, fluvial derived sedimentation in Chapman Pond following the late 1800s is concurrent with the opening of the main inlet to the pond (i.e. the Great Ditch), and provides strong evidence for a connection. Further, the radiocarbon date obtained below a similar sudden shift to lower organics at Pecausett Pond supports an order-of-magnitude increase in the rate of deposition at this ~1900 CE transition. It is possible that the sudden change in age above and below this organic transition may indicate an erosional hiatus, which could potentially explain age discrepancies for the Hg onset between the floodplain waterbodies and past results by Varekamp et al. (2003). However, floodplain waterbodies in the study are extremely sheltered, limiting the mechanisms capable of substantial erosion, other than by way of a redirection of the main river. Pecausett Pond is identified in maps dating as far back as the late 1700 s (Blodget, 1792), with no documentation for the main river meandering into the pond since detailed records began during colonial times. Historical accounts, however, do indicate efforts to improve the tidal flushing capacity of the pond with drainage ditches in the marsh and probably also the clearing of the main inlet around the time period of the organic transition in PCT1. The timing of the clearing of the main inlet to Chapman Pond (and likely Pecausett Pond as well), is also cotemporaneous with the dredging of the main navigation channel at Hamburg Cove. Major man-made alterations therefore occurred at each of the three tidal floodplain waterbodies around the turn of the 19th century, with rapid rates of infilling probably induced by these modifications.

Without the routine removal of tree jams to allow access to off-river harbors and popular fishing holes; tie-channels become obstructed, preventing the introduction of river water to these backwater locations. However, prior to colonization clogging debris was rarely cleared, and secondary man-made channels did not exist. Thus, human impacts have likely resulted in a vast array of active tidal off-river waterbodies, with significantly enhanced accommodation space in the tidal river for sediment storage, as compared to the purely natural state, where only a few tidal off-river waterbodies would be active at any given time. However, the lifespan of these valued tidal backwater environments is likely limited, as the unhindered deposition of sediment will eventually fill these ponds to their maximal capacity over the next century. The rapid rates of infilling of these waterbodies is therefore likely unusual for a “natural” system, yet potentially common for many tidal rivers on the Atlantic East Coast due to the anthropogenic creation and maintenance of tidal tie-channels over the last few centuries.

6.4. Enhanced trapping of pollutants

Results presented in Fig. 3 indicate that floodplain waterbodies along the Connecticut River contain some of the highest concentrations of heavy metal contamination within the entire Connecticut River/Long Island Sound system. Concentrations exceed 3600 ppb at Hamburg Cove, nearly an order of magnitude greater than the peak concentrations of 409 ppb in neighboring Great Island Marsh. For perspective, Hg levels in HMB1 are over three times typical peak concentrations observed in San Francisco Bay (790 ppb, Conaway et al.,

2008), which is often highlighted prominently as a top case of legacy Hg contamination in the United States. By comparison, off-river waterbodies such as Chapman Pond appear relatively pristine (distinctions of note for the Connecticut River include it being one of only 26 U.S. wetlands recognized for international significance by the United Nations Ramsar Convention, and among 40 of the 'Last Great Places' in the Western Hemisphere as designated by the Nature Conservancy).

It is possible that the initial rapid rise in Hg observed at Chapman Pond and Pecausett Pond is due to observed changes in sediment lithology (e.g. Fig. 6). However, Hg preferentially associates with organics rather than clastic material (e.g. Huang et al., 1996). The initial rise in Hg just above the observed sudden drop in organics is therefore inconsistent with this mechanism. Chapman Pond and Pecausett Pond are both located well above the salinity reach, thus the rapid rise in Hg is not caused by the enhancement of heavy metals on sediments by the mixing of fresh and seawater. The onset of Hg contamination in PCT1 also occurs ~30–70 cm above the shift to less organic sediments (Fig. 6B), with Hg concentrations remaining relatively low through this organic transition. Significant variability in Hg is also observed above the industrial onset for Hg PCT1 and CMP3, including the 1950–1970 CE peak in Hg, which occurs at depths where organic content remains relatively constant down-core (Fig. 6). Variability in Hg therefore appears to be linked less with changes in sediment lithology, and more consistent with a reflection of time-varying changes in Hg introduction to the environment due to industrial related activities along the main river (Varekamp et al., 2003, 2005). Man-made alterations to tie-channels at the turn of the last century therefore appear to have enhanced sediment trapping in tidal floodplain waterbodies at the opportune time to capture industrial contaminants as they began entering the environment at unprecedented levels.

7. Conclusions

The tidal reach of many lowland river systems often extends upriver 100 km or more. Cut-off meanders, backwater ponds, and blocked valley coves are all prominent features along this tidal reach. Results from this study provide new information for how sediment is distributed within these floodplain systems:

1. Floodplain lakes and coves on the Connecticut River exhibit extremely high deposition rates when compared to neighboring floodplain environments. These slack-water environments also exhibit a clear seaward increase in deposition towards the mouth of the tidal river. Suspended sediments from the main river are transported into tidal off-river waterbodies via tie-channels during each flood tide, with a majority of this sediment settling out before it can be exported by ebbing flows. Increases in sediment accumulation with growing tidal influence indicate that this process of tidal pumping plays a key role in the trapping of sediment within backwater sites on the floodplain of tidal rivers.
2. Rates of deposition within tidal off-river waterbodies appear to have remained relatively steady over the last century, with little evidence for thick sedimentary units of similar age that would point towards sedimentation driven episodically by extreme events. Tides diminish significantly along most of the river during periods of abnormally high river discharge, with most material bypassing backwater sites during these extreme events. As a result, trapping in tidal off-river waterbodies occurs predominantly during more moderate flooding conditions.
3. Once a tidal tie-channel is established (either naturally or by human intervention), the associated floodplain pond or cove quickly infills with sediment. The creation and routine maintenance of inlets connecting off-river waterbodies to the main channel have likely increased both the distribution and connectivity of these systems to the tidal river in recent centuries. Thus, the relative role of tidal off-river waterbodies in storing floodplain sediments has increased substantially in managed tidal river systems like the Connecticut.
4. In the case of the Connecticut River, the human maintenance of inlets begins at the onset of industrialization — at a time when contaminants were being introduced to the river at unprecedented levels. As a consequence, a network of tidal off-river waterbodies was initiated at the most favorable time for the trapping and storage of legacy contaminants.

Acknowledgments

J.D. Woodruff gratefully acknowledges support from the National Science Foundation (EAR-1158780, EAR-1148244 and IF-0949313), as well as funds provided by a Faculty Research Grant/Healey Endowment Grant from the University of Massachusetts and USGS WRRA Grant #2011MA298B. This work benefited greatly through field and lab assistance by N. Gayer, C. Rothacker, N. Sanches, and C. Sullivan from Amherst College with funding from the Hitchcock Environmental Science Fund. E. Catabriani, L. Geiger, K. Jacobacci, G. Romano and J. Schneider also provide valuable support in the field during their Keck Geology Consortium summer research under the direction of S. O'Connell and P. Patton from Wesleyan University.

References

Aalto, R., Lauer, J., Dietrich, W., 2008. Spatial and temporal dynamics of sediment accumulation and exchange along Strickland River floodplains (Papua New Guinea) over decadal-to-centennial timescales. Journal of Geophysical Research 113.
Allison, M., Kuehl, S., Martin, T., Hassan, A., 1998. Importance of flood-plain sedimentation for river sediment budgets and terrigenous input to the oceans: insights from the Brahmaputra-Jamuna River. Geology 26, 175.
Appleby, P., Oldfield, F., 1978. The calculation of lead-210 dates assuming a constant rate of supply of unsupported 210Pb to the sediment. Catena 5, 1–8.
Bissell, M., 1925. Preglacial course of the Connecticut River near Middletown, Connecticut, and its significance. American Journal of Science 5, 233.
Blodget, W., 1792. A New and Correct Map of Connecticut: One of the United States of North America from Actual Survey, Humbly Dedicated by Permission to his Excellency Samuel Huntington Esquire Governor and Commander in Chief of Said State/ by his Most Humble Servant William Blodget., Middletown, CT.
Boldt, K.V., Lane, P., Woodruff, J.D., Donnelly, J.P., 2010. Calibrating a sedimentary record of overwash from Southeastern New England using modeled historic hurricane surges. Marine Geology 275, 127–139.
Bourn, W.S., Cottam, C., 1950. Some biological effects of ditching tidewater marshes. In: U.S.D. Fish and Wildlife Service, o. Interior (Eds.), Washington, DC, USA.
Bubb, J.M., Rudd, T., Lester, J.N., 1991. Distribution of heavy metals in the River Yare and its associated broads I. Mercury and methylmercury. The Science of the Total Environment 102, 147–168.
Bubb, J., Williams, T., Lester, J., 1993. The behaviour of mercury within a contaminated tidal river system. Water Science and Technology 28, 329–338.
Buck, C.E., Millard, A., 2004. Tools for Constructing Chronologies: Crossing Disciplinary Boundaries, 177. Springer Verlag.
Chen, Z., Saito, Y., Kanai, Y., Wei, T., Li, L., Yao, H., Wang, Z., 2004. Low concentration of heavy metals in the Yangtze estuarine sediments, China: a diluting setting. Estuarine, Coastal and Shelf Science 60, 91–100.
Citterio, A., Piègay, H., 2009. Overbank sedimentation rates in former channel lakes: characterization and control factors. Sedimentology 56, 461–482.
Conaway, C.H., Black, F.J., Grieb, T.M., Roy, S., Flegal, A.R., 2008. Mercury in the San Francisco estuary. Reviews of Environmental Contamination and Toxicology 29–54.
Constantine, J.A., Dunne, T., PiÈgay, H., Mathias Kondolf, G., 2010. Controls on the alluviation of oxbow lakes by bed material load along the Sacramento River, California. Sedimentology 57, 389–407.
Day, G., Dietrich, W., Rowland, J., Marshall, A., 2008. The depositional web on the floodplain of the Fly River, Papua New Guinea. Journal of Geophysical Research 113.
Dean, W.E., 1974. Determination of carbonate and organic matter in calcareous sediments and sedimentary rocks by loss on ignition: comparison with other methods. Journal of Sedimentary Petrology 44, 242–248.
Donnelly, J.P., Woodruff, J.D., 2007. Intense hurricane activity over the past 5,000 years controlled by El Niño and the West African monsoon. Nature 447, 465–468.
Duffield, W.W., 1895. Connecticut River: Higganum to Rocky Hill, Connecticut. U.S. Coast and Geodetic Survey, Washington, D.C.
Faure, G., 1986. Principles of Isotope Geology, Second edition. John Wiley and Sons, U.S.A.
Feng, H., Cochran, J.K., Hirschberg, D.J., 1999. Th-234 and Be-7 as tracers for the sources of particles to the turbidity maximum of the Hudson River estuary. Estuarine, Coastal and Shelf Science 49, 629–645.
Ferguson, R.I., Church, M., 2004. A simple universal equation for grain settling velocity. Journal of Sedimentary Research 74, 933–937.

Galler, J., Allison, M., 2008. Estuarine controls on fine-grained sediment storage in the Lower Mississippi and Atchafalaya Rivers. Geological Society of America Bulletin 120, 386.
Garvine, R., 1975. The distribution of salinity and temperature in the Connecticut River estuary. Journal of Geophysical Research 80, 1176–1183.
Geyer, W.R., Woodruff, J.D., Traykovski, P., 2001. Sediment transport and trapping in the Hudson River estuary. Estuaries 24, 670–679.
Goodbred Jr., S., Kuehl, S., 1998. Floodplain processes in the Bengal Basin and the storage of Ganges-Brahmaputra river sediment: an accretion study using 137Cs and 210Pb geochronology. Sedimentary Geology 121, 239–258.
Groner, M., Thomas, E., Varekamp, J., 2004. Radiocarbon studies of Long Island sound sediments. American Geophysical Union, Spring Meeting, Montreal, Canada.
Hageman, B., 1969. Development of the western part of the Netherlands during the Holocene. Geologie en Mijnbouw 48, 373–388.
Holland, M.M., Burk, J.C., 1982. Relative ages of western Massachusetts Oxbow Lakes. Northeastern Geology 4, 23–32.
Horne, G., Patton, P., 1989. Bedload-sediment transport through the Connecticut River estuary. Geological Society of America Bulletin 101, 805.
Howard-Strobel, M., O'Donnell, J., Bohlen, W., Cohen, D., 1996. Observations on the hydrography of the Connecticut River during high and low river discharges. In: Van Patten, M.S. (Ed.), Long Island Sound Research Conference. Connecticut Sea Grant, University of Connecticut, pp. 32–44.
Huang, C., Allen, H.E., Yin, Y., Sanders, P.F., Li, Y., 1996. Adsorption of mercury (II) by soil: effects of pH, chloride, and organic matter. Journal of Environmental Quality 25, 837–844.
Jacobs, R.P., O'Donnell, E.B., 2003. A fisheries Guide to Lakes and Ponds of Connecticut, Including the Connecticut River and its Coves, DEP Bulletin 35. Connecticut Department of Environmental Protection, Hartford, CT.
Klingbeil, A., Sommerfield, C., 2005. Latest Holocene evolution and human disturbance of a channel segment in the Hudson River Estuary. Marine Geology 218, 135–153.
Koide, M., Bruland, K.W., Goldberg, E.D., 1973. Th228/Th232 and Pb210 geochronologies in marine and lake sediments. Geochimica et Cosmochimica Acta 37, 1171–1188.
Kratz, L.N., Woodruff, J.D., Martini, A.M., Morrison, J., 2012. Resultant Sedimentation from tropical storm Irene in the Lower Connecticut River, Northeastern Section, GSA. 47th Annual Meeting, Hartford, CT. USA.
Larsen, F.D., Cutshall, N.H., 1981. Direct determination of Be-7 in sediments. Earth and Planetary Science Letters 54, 379–384.
Lemieux, C.R., 1983. Suspended Sediment Tranport in the Connecticut River Estuary. B.S., Wesleyan University, Middletown, CT. (112 pp.).
Loomis, M.J., Craft, C.B., 2010. Carbon sequestration and nutrient (nitrogen, phosphorus) accumulation in river-dominated tidal marshes, Georgia, USA. Soil Science Society of America Journal 74, 1028–1036.
Maloney, T., Barrett, J.P., Council, C.R.W., 2001. Tidewaters of the Connecticut River. River's End Press.
Meade, R., 1982. Sources, sinks, and storage of river sediment in the Atlantic drainage of the United States. Journal of Geology 90, 235–252.
Mertes, L., 1994. Rates of flood-plain sedimentation on the central Amazon River. Geology 22, 171.
Milliman, J.D., Farnsworth, K.L., 2011. River Discharge to the Coastal Ocean: a Global Synthesis. Cambridge University Press, Cambridge.
Nash, D.B., 1994. Effective sediment-transporting discharge from magnitude-frequency analysis. Journal of Geology 79–95.
NOAA, 2012. Tide data for Connecticut River, Stations #8462925, #8463836, #8464336. NOAA/NOS/CO-OPS.
Olsen, C.B., Larsen, I.L., Lowry, P.D., Cutshall, N.H., Nichols, M.M., 1986. Geochemistry and deposition of Be-7 in river-estuarine and coastal waters. Journal of Geophysical Research 91, 896–908.
Patton, P.C., Horne, G.S., 1992. Response of the Connecticut River estuary to late Holocene sea level rise. Geomorphology 5, 391–417.
Paola, C., Voller, V., 2005. A generalized Exner equation for sediment mass balance. Journal of Geophysical Research 110, F04014.
Pennington, W., Cambray, R.S., Fischer, E., 1973. Observations on lake sediments using fallout Cs-137 as a tracer. Nature 242, 324–326.
Plater, A., Kirby, J., 2006. The potential for perimarine wetlands as an ecohydrological and phytotechnological management tool in the Guadiana estuary, Portugal. Estuarine, Coastal and Shelf Science 70, 98–108.
Ralston, D.K., Geyer, W.R., 2009. Episodic and long-term sediment transport capacity in the Hudson River estuary. Estuaries and Coasts 32, 1130–1151.
Redfield, A., 1972. Development of a New England salt marsh. Ecological Monographs 42, 201–237.
Reimer, P., Baillie, M., Bard, E., Bayliss, A., Beck, J., Blackwell, P., Ramsey, C.B., Buck, C., Burr, G., Edwards, R., 2009. IntCal09 and Marine09 radiocarbon age calibration curves, 0–50,000 years cal BP. Radiocarbon 51, 1111–1150.
Reimers, R., Krenkel, P., 1974. Kinetics of mercury adsorption and desorption in sediments. Journal Water Pollution Control Federation 46, 352–365.
Robbins, J.A., Edgington, D.N., 1975. Determination of recent sedimentation rates in Lake Michigan using Pb-210 and Cs-137. Geochimica et Cosmochimica Acta 39, 285–304.
Rowland, J., Lepper, K., Dietrich, W., Wilson, C., Sheldon, R., 2005. Tie channel sedimentation rates, oxbow formation age and channel migration rate from optically stimulated luminescence (OSL) analysis of floodplain deposits. Earth Surface Processes and Landforms 30, 1161–1179.
Rozsa, R., 1995. Human impacts on tidal wetlands: history and regulations. In: Dreyer, G.D., Niering, W.A. (Eds.), Tidal Marshes of Long Island Sound: Ecology, History and Restoration. The Connecticut Arboretum Press, New London, CT, USA, pp. 42–50.
Schuler, S. (Ed.), 1993. Hamburg Cove: Past and Present: Florence Griswold Museum.
Simpson, R.L., Good, R.E., Leck, M.A., Whigham, D.F., 1983. The ecology of freshwater tidal wetlands. Bioscience 33, 255–259.
Swanson, K., Watson, E., Aalto, R., Lauer, J., Bera, M., Marshall, A., Taylor, M., Apte, S., Dietrich, W., 2008. Sediment load and floodplain deposition rates: comparison of the Fly and Strickland rivers, Papua New Guinea. Journal of Geophysical Research 113.
Traykovski, P., Geyer, R., Sommerfield, C., 2004. Rapid sediment deposition and fine-scale strata formation in the Hudson estuary. Journal of Geophysical Research 109, F02004.
Trimble, S., 1983. A sediment budget for Coon Creek basin in the Driftless Area, Wisconsin, 1853–1977. American Journal of Science 283, 454.
Varekamp, J., Kreulen, B., ten Brink, B., Mecray, E., 2003. Mercury contamination chronologies from Connecticut wetlands and Long Island Sound sediments. Environmental Geology 43, 268–282.
Varekamp, J., Mecray, E., Maccalous, T., 2005. Once spilled, still found: metal contamination in Connecticut coastal wetlands and Long Island Sound sediment from historic industries. In: Whitelaw, D.M., Visgilio, G.R. (Eds.), America's Changing Coasts: Private Rights and Public Trust. Edward Elgar Publishing, Northampton, MA, pp. 122–147.
Walling, H.F., 1856. A Topographical Map of Hampshire County, Massachusetts. Liht of Sargony & Co, New York, New York.
Walling, H.F., 1859. Map of Middlesex County, Connecticut. H. & C.T. Smith & Co., New York, NY.
Walling, D., 2003. Using environmental radionuclides as tracers in sediment budget investigations. In: Bogen, J., Fergus, T., Walling, D. (Eds.), Erosion and Sediment Tranport Measurements in Rivers: Technological and Methodological Advances. International Association of Hydrological Sciences, Oxfordshire, UK, pp. 57–78.
Walling, D., Owens, P., Leeks, G., 1998. The role of channel and floodplain storage in the suspended sediment budget of the River Ouse, Yorkshire, UK. Geomorphology 22, 225–242.
Walling, D., Owens, P., Leeks, G., 1999. Rates of contemporary overbank sedimentation and sediment storage on the floodplains of the main channel systems of the Yorkshire Ouse and River Tweed, UK. Hydrological Processes 13, 993–1009.
Walling, D., Owens, P., Carter, J., Leeks, G., Lewis, S., Meharg, A., Wright, J., 2003. Storage of sediment-associated nutrients and contaminants in river channel and floodplain systems. Applied Geochemistry 18, 195–220.
Wolman, M.G., Miller, J.P., 1960. Magnitude and frequency of forces in geomorphic processes. Journal of Geology 68, 54–74.
Woodruff, J.D., 1999. Sediment Deposition in the Lower Hudson River Estuary. M.S., Massachusetts Institute of Technology and Woods Hole Oceanographic Institution. (57 pp.).
Woodruff, J.D., Geyer, W.R., Sommerfield, C.K., Driscoll, N.W., 2001. Seasonal variation of sediment deposition in the Hudson River estuary. Marine Geology 179, 105–119.
Woodruff, J.D., Donnelly, J.P., Mohrig, D., Geyer, W.R., 2008. Reconstructing relative flooding intensities responsible for hurricane-induced deposits from Laguna Playa Grande, Vieques, Puerto Rico. Geology 36, 391–394.
Woodruff, J.D., Donnelly, J.P., Okusu, A., 2009. Exploring typhoon variability over the mid-to-late Holocene: evidence of extreme coastal flooding from Kamikoshiki, Japan. Quaternary Science Reviews 28, 1774–1785.